

**NEON AND HELIUM IN THE SURFACE OF STARDUST CELL C2028.** R. L. Palma<sup>1,2</sup>, R. O. Pepin<sup>1</sup>, D. J. Schlutter<sup>1</sup>, D. R. Frank<sup>3</sup>, R. Bastien<sup>3</sup>, and M. Rodriguez<sup>3</sup>, <sup>1</sup>Department of Physics, University of Minnesota, Minneapolis, MN 55455, USA, <sup>2</sup>Department of Physics & Astronomy, Minnesota State University, Mankato, MN 56001, USA: [russell.palma@mnsu.edu](mailto:russell.palma@mnsu.edu), <sup>3</sup>ESCG, NASA Johnson Space Center, Houston, TX 77058, USA.

**Introduction:** Previous studies of light noble gases in Stardust aerogel samples detected a variety of isotopically non-terrestrial He and Ne compositions [1-4]. However, with one exception, in none of these samples was there visible evidence for the presence of particles that could have hosted the gases. The exception is materials keystoneed from track 41, cell C2044, which contained observable fragments of the impacting Wild 2 comet coma grain [2]. Here we report noble gas data from a second aerogel sample in which grains are observed, cut from the surface of a cell (C2028) riddled with tiny tracks and particles that are thought to be secondary in origin, ejected toward the cell when a parent grain collided with the spacecraft structure and fragmented. Interestingly, measured  $^{20}\text{Ne}/^{22}\text{Ne}$  ratios in the track 41 and C2028 samples are similar, and within error of the meteoritic “Q-phase” Ne composition [5].

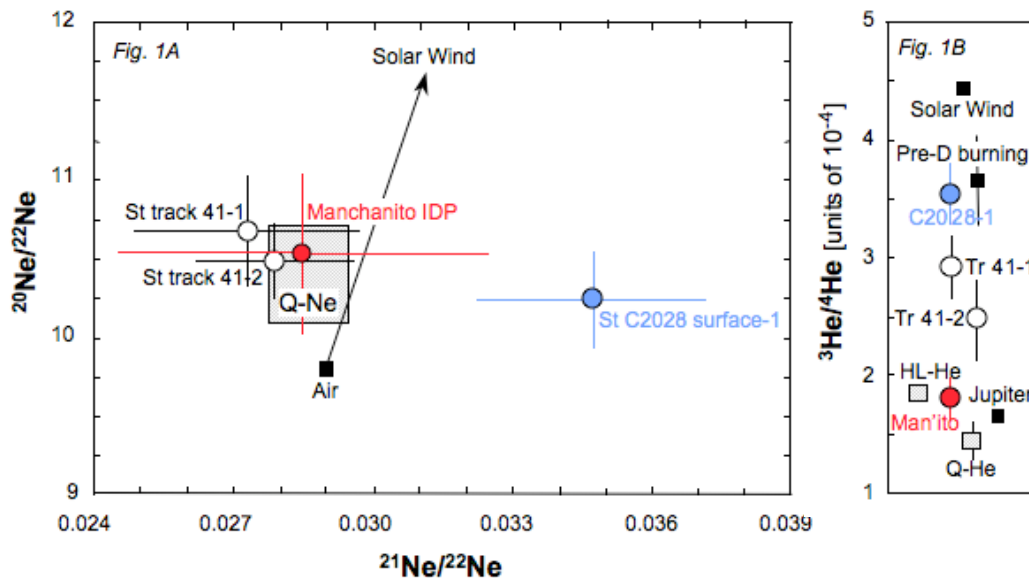
**Experimental:** The surface of cell C2028 in the Stardust comet tray was scanned by high-resolution zoom-focus movies [6] at the JSC Stardust Curatorial Facility to assay its population of small particle tracks. The  $\sim 770$  movies, each with a  $480\mu\text{m} \times 360\mu\text{m}$  field of view, collectively imaged  $\sim 130\text{mm}^2$ , about 17% of the cell surface area. The scans revealed a track density of  $\sim 1$  per  $\text{mm}^2$  of surface area. Tracks averaged  $\sim 50\mu\text{m}$  in length and contained embedded terminal particles roughly  $1\mu\text{m}$  in diameter. Track axes were off-normal to the cell surface and pointed toward the spacecraft’s Whipple shield, indicating that the terminal particles are secondary fragments ejected during collision of a coma grain with the shield [7].

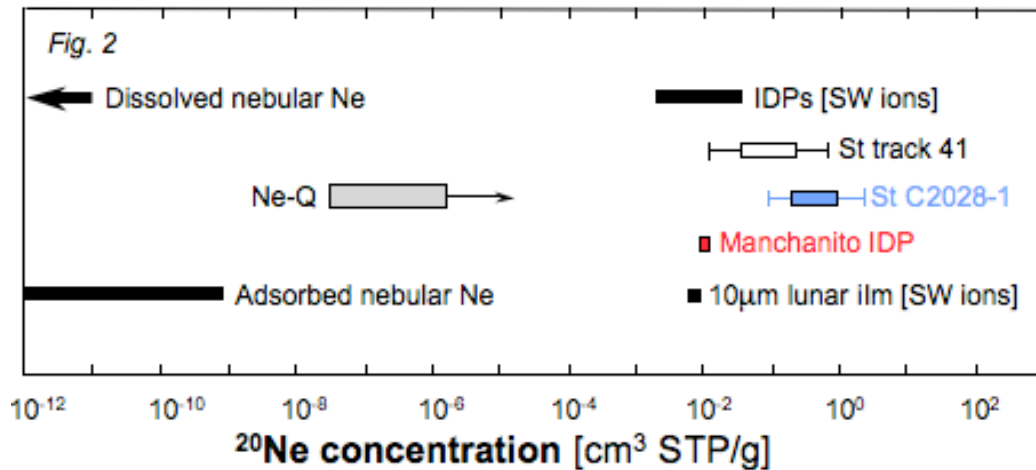
Noble gas analyses were carried out on aerogel samples  $\sim 100\mu\text{m}$  thick and  $\sim 0.5\text{cm}^2$  in area keystoneed from the C2028 surface, crushed and loaded in Pt foils, and degassed by step-heating to  $\sim 1400^\circ\text{C}$ . Details of the mass spectrometry and experimental protocol used in the He and Ne measurements are given in [8].

**Results:**  $^{20}\text{Ne}/^{22}\text{Ne}$ . The Ne composition measured in the C2028 cell surface is shown in Figs. 1A, and compared to compositions found in Stardust track 41 [2] and the “Manchanito” particle from the L2071F1 cluster IDP [9]. All three display  $^{20}\text{Ne}/^{22}\text{Ne}$  ratios (Fig. 1A) that fall within the Q-Ne data field [5].

$^3\text{He}/^4\text{He}$ . The He ratio is elevated with respect to  $\text{Q-}^3\text{He}/^4\text{He}$  in both Stardust samples (Fig. 1B), suggesting the presence of solar wind (SW) components. The possible presence of SW-He in the analyzed track 41 materials was considered by [2 (SOM)], and  $^3\text{He}/^4\text{He}$  ratios resembling SW have been seen in surface samples adjacent to track 41 [4]. The higher  $^3\text{He}/^4\text{He}$  in C2028 (Fig. 1B) arguably reflects additions of both SW-He and a spallogenic  $^3\text{He}$  component to an initially Q-like  $^3\text{He}/^4\text{He}$  ratio.

$^{20}\text{Ne}$  concentration. Fig. 2, discussed in [2] and updated for this study, shows the approximate Ne loading of the C2028 particles, obtained by dividing its measured abundance by the estimated grain mass present in the  $0.5\text{cm}^2$  sample area. Based on the movie scan data, the grain mass assumed here is that of 50 particles ( $1/\text{mm}^2$ ) with an average diameter of  $1\mu\text{m}$ ; the blue box in Fig. 2 represents the concentration variation for grain densities ranging from 1 to  $4\text{g}/\text{cm}^3$ .



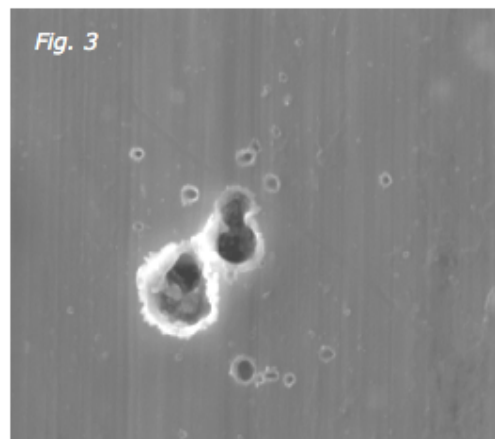


Other mass estimate uncertainties are noted below.

**Discussion:** The Q-Ne composition, hosted in a minor but gas-rich macromolecular organic phase ubiquitous in chondritic and achondritic meteorites [5], appears not to be confined to meteoritic “phase-Q”. A Q- $^{20}\text{Ne}/^{22}\text{Ne}$  signature has now been seen in two Wild 2 comet coma samples, in the Manchanito IDP, and most recently in several grains from the U2-20GCA giant cluster IDP [10]. In none of these is there evidence, as yet, that the Q-Ne carriers are carbonaceous.

A striking difference between the two comet samples is the elevated  $^{21}\text{Ne}/^{22}\text{Ne}$  ratio in C2028 (Fig. 1A), pointing to a spallation component. As noted above, the high  $^3\text{He}/^4\text{He}$  in C2028 (Fig. 1B) could also be due, in part, to spallogenic He. The calculated spallation  $^{21}\text{Ne}$  concentration is large,  $\sim 2 \times 10^{-4}$  ccSTP/g. Division by a production rate appropriate to space irradiation of small grains [11] leads to an impossibly long exposure age unless particle exposure occurred near the young evolving sun in an environment of intense flare-generated radiation before their transport to comet-forming nebular regions, as discussed in [10].

The principal uncertainty in the Ne loading plotted in Fig. 2 is the mass of the grains—assumed to be the gas carriers—embedded in the C2028 sample. Other factors, aside from their unknown densities, are in play. The right error bar reflects the possibility that the particles are coated with melted aerogel to the extent that their actual diameters are only half their average imaged size. The left limit is based on observations of crater populations in Al foil exposed to particle impacts on the comet dust collector [12]. One feature, shown in Fig. S5 in [12], is reproduced in Fig. 3. Its crater distribution of descending sizes is interpreted by [12] as impacts of a recently disaggregated small parent particle. From crater-projectile size scaling the largest impactor was a  $\sim 1\mu\text{m}$  grain, comparable to the C2028 particles. But about half the total mass in the fragmentation debris field is carried by secondary fragments less than  $\sim 0.5\mu\text{m}$  in size. These might have survived a similar impact into aerogel, but were generally too small to create tracks detectable at the resolution of the



movie scans. This estimate of C2028 sample mass, marked by the end of the left error bar in Fig. 2, may be the preferable choice for  $^{20}\text{Ne}$  concentration. Other possibilities include a density of secondary tracks and particles well above  $\sim 1/\text{mm}^2$  in the area from which the C2028 sample was taken, which was not scanned. However a high track density, and a presence of larger particles which would severely increase the estimated mass, would have been observed during keystoneing.

These mass uncertainties, while large, are still too small to challenge the conclusion that the high Ne concentration in C2028, overlapping Stardust track 41 and falling in the same area of Fig. 2 as Manchanito, is due to Q-Ne ion implantation [2,9]. This mechanism produces the similarly large Ne loadings of SW-irradiated IDPs and lunar ilmenites shown in Fig. 2.

**References:** [1] Palma R. L. et al. (2007) *LPSC 38<sup>th</sup>*, #2032. [2] Marty B. et al. (2008) *Science* 319, 75. [3] Palma R. L. et al. (2012) *LPSC 43<sup>rd</sup>*, #1076. [4] Palma R. L. et al. (2013) *LPSC 44<sup>th</sup>*, #1084. [5] Busemann H. et al. (2000) *Meteorit. Planet. Sci.* 35, 949. [6] Westphal A. J. et al. (2014) *Meteorit. Planet. Sci.* 49, 1509. [7] Westphal A. J. et al. (2006) *Meteorit. Planet. Sci.* 43, 415. [8] Pepin R. O. et al. (2011) *ApJ* 742:86. [9] Palma R. L. et al. (2013) *LPSC 44<sup>th</sup>*, #1694. [10] Pepin R. O. et al. (2015), this conference. [11] Reedy R. C. (1987) *Proc. 17th LPSC, Part 2*, E697. [12] Hörz F. et al. (2006) *Science* 314, 1716.